

Article

# Plant-Based Substrates for the Production of Iron Bionanoparticles (Fe-BNPs) and Application in PCB Degradation with Bacterial Strains

Marcela Tlčíková<sup>1,\*</sup> , Hana Horváthová<sup>1,2</sup> , Katarína Dercová<sup>3</sup>, Michaela Majčinová<sup>3</sup>, Mariana Hurbanová<sup>3</sup>, Katarína Turanská<sup>3</sup> and Ľubomír Jurkovič<sup>1</sup>

<sup>1</sup> Department of Geochemistry, Faculty of Natural Sciences, Comenius University in Bratislava, Ilkovičova 6, 842 15 Bratislava, Slovakia; hana.horvathova@uniba.sk (H.H.); lubomir.jurkovic@uniba.sk (L.J.)

<sup>2</sup> The Centre of Environmental Services, Ltd., Kutlíkova 17, 852 50 Bratislava, Slovakia

<sup>3</sup> Institute of Biotechnology, Faculty of Chemical and Food Technology, Slovak University of Technology Bratislava, Radlinského 9, 812 37 Bratislava, Slovakia; katarina.dercova@stuba.sk (K.D.)

\* Correspondence: tlcikova2@uniba.sk

**Abstract:** Removing polychlorinated biphenyls (PCBs) from the environment is an important process for the protection of biota. This work examines three different approaches to the degradation of such contaminants. The first involves the use of iron bionanoparticles (Fe-BNPs) prepared through green synthesis from selected plant matrices. The second approach entails the use of the bacteria *Stenotrophomonas maltophilia* (SM) and *Ochrobactrum anthropi* (OA) isolated from a PCB-contaminated area, Strážsky canal, located in the Slovak republic, which receives efflux of canal from Chemko Strážske plant, a former producer of PCB mixtures. The third approach combines these two methods, employing a sequential hybrid two-step application of Fe-BNPs from the plant matrix followed by the application of bacterial strains. Fe-BNPs are intended to be an eco-friendly alternative to synthetic nanoscale zero-valent iron (nZVI), which is commonly used in many environmental applications. This work also addresses the optimization parameters for using nZVI in PCB degradation, including the pH of the reaction, oxygen requirements, and dosage of nZVI. Pure standards of polyphenols (gallic acid, GA) and flavonoids (quercetin, Q) were tested to produce Fe-BNPs using green synthesis at different concentrations (0.1, 0.3, 0.5, 0.8, and 1 g.L<sup>-1</sup>) and were subsequently applied to the PCB degradation experiments. This step monitored the minimum content of bioactive substances needed for the synthesis of Fe-BNPs and their degradation effects. Experimental analysis indicated that among the selected approaches, sequential nanobiodegradation appears to be the most effective for PCB degradation, specifically the combination of Fe-BNPs from sage and bacteria SM (75% degradation of PCBs) and Fe-BNPs from GA (0.3 g.L<sup>-1</sup>) with bacteria OA (92% degradation of PCBs).

**Keywords:** bionanoparticles; green synthesis; nanobiodegradation; PCB; bacteria



**Citation:** Tlčíková, M.; Horváthová, H.; Dercová, K.; Majčinová, M.; Hurbanová, M.; Turanská, K.; Jurkovič, Ľ. Plant-Based Substrates for the Production of Iron Bionanoparticles (Fe-BNPs) and Application in PCB Degradation with Bacterial Strains. *Processes* **2024**, *12*, 1695. <https://doi.org/10.3390/pr12081695>

Academic Editor: Adina Musuc

Received: 16 July 2024

Revised: 3 August 2024

Accepted: 12 August 2024

Published: 13 August 2024



**Copyright:** © 2024 by the authors. Licensee MDPI, Basel, Switzerland. This article is an open access article distributed under the terms and conditions of the Creative Commons Attribution (CC BY) license (<https://creativecommons.org/licenses/by/4.0/>).

## 1. Introduction

Polychlorinated biphenyls (PCBs) are synthetic compounds with 1–10 chlorines per molecule. They belong to the group of persistent organic pollutants (POPs), known for their harmful properties. Czechoslovakia began producing PCBs in the late 1950s at the industrial chemical plant Chemko Strážske and ceased production in 1984. Almost 40 years after the production ban, the wide area around the plant remains extensively contaminated by PCBs [1]. In January 2020, a state of emergency was declared in the area, and barrels with solid PCB residues, left unsecured around the Chemko plant, were moved into shipping containers to remove the source of the contamination. However, leaked PCBs persist in the soil and river sediments. Remediation of PCB-contaminated sites is essential to minimize human exposure and environmental risks. Commonly used technologies for this purpose include chemical oxidation/reduction, solvent extraction, base-catalyzed decomposition

(BCD), bioremediation, and phytoremediation [2–4]. One potential method of removing such PCBs is the use of nanotechnology. Recently, nanoscale zero-valent iron (nZVI) has been widely used as an effective contaminant degrader due to its high reactivity and large specific surface area [5]. Nanoscale zero-valent iron eliminates PCBs predominantly through a reduction mechanism - reducing dehalogenation [6]. It can be produced by a chemical or physical processes, neither of which are completely environmentally acceptable methods [7]. An alternative method to synthesize Fe-based nanoparticles (Fe-BNPs) via green synthesis, which is cheaper, environmentally friendly, and does not produce toxic substances. This method involves using a natural resource as a matrix and a metal salt, which interacts with the bioactive substances contained in the matrix. After synthesis, single-component metal Fe-BNPs are formed. Their shape and size depend on the input material, preparation conditions, and synthesis duration [8]. The green synthesis method used in this paper is a type of phytonanotechnology based on the use of various plant matrices. The matrices used in synthesis should contain polyphenols, a key component of nanoparticle synthesis, but also lipids, proteins, vitamins, and various other organic molecules that serve as carriers of the OH- group and react [9]. Representative polyphenols include gallic acid (GA), which, due to its reducing and stabilizing properties, can be used for Fe-BNPs synthesis [10]. A representative flavonoid (a polyphenol subgroup), quercetin (Q), possesses similar properties. Polyphenols containing hydroxyl or carbonyl groups form complexes with added metal salts, which are subsequently reduced to zero-valent iron according to Equation (1) [11]: (*Ar*-aromatic ring)



Equation (1) represents one potential method of iron bionanoparticle formation. Other studies suggest that gallates or catechols react with iron salt to form chelates, leading to octahedral network formation [12]. The color change of the reaction mixture from dark brown to black indicates an ongoing reaction between bioactive substances and iron [13]. A sequential or combined method of PCB degradation using synthetic nanoparticles or Fe-BNPs and bacterial cultures naturally adapted to the contaminant can provide higher efficiency in removing harmful substances from the environment [14]. Remediation of contaminated areas using only one remediation technology can be costly and inefficient. Consequently, the development of integrated processes involving the application of two or more technologies is essential.

Nanobioremediation is a hybrid remediation technology combining nanomaterials and bioremediation to remove contaminants [15]. It is an approach tailored to the chemical structure of PCBs. The integration of abiotic and biotic degradation is based on the anaerobic dechlorination of highly-chlorinated PCBs using nZVI or Fe-BNPs, and the subsequent aerobic degradation of the lower-chlorinated PCBs or biphenyl using bacteria and their enzymes [16]. The major presumed mechanism of PCB degradation using Fe-BNPs is adsorption, with reduction playing a minor role. The disadvantage of solely microbial degradation is that only a few microbial cultures are capable of dechlorinating PCB mixtures, and, generally, these methods require a long time for complete mineralization, i.e., degradation to inorganic salts, CO<sub>2</sub>, and H<sub>2</sub>O [16]. Moreover, high concentrations of contaminants can have a toxic effect on selected remedial microorganisms [15]. Combining nanotechnology and biotechnology can overcome the limitations of both methods [17]. The dimensions of nZVI allow better mobility through porous media, thereby enhancing the remediation process without altering the original properties of the media. Consequently, subsequent application of processes such as bioremediation can serve as a supportive method without requiring changes or additional adjustments in situ [18]. The advantage of combination these two methods is an expected increase in PCB degradation. Nanoparticles alone (nanoremediation) cannot degrade the biphenyl ring, leading to biphenyl accumulation in the environment, while bacterial strains alone (bioremediation) may not extensively dechlorinate highly chlorinated PCB congeners, possibly due to partial toxicity and steric effects. Therefore, the sequential combination of these methods appears highly appropriate.

This presented study focuses on (a) screening plant-based substrates to produce iron bionanoparticles and their application in PCB nanodegradation, (b) the biodegradation of PCBs using isolated bacteria adapted to PCBs, and (c) a combined approach for potentially increased PCB degradation, representing a sequential hybrid degradation called nanobiodegradation.

## 2. Materials and Methods

### 2.1. Sample Preparation

#### 2.1.1. Ethanol Extract of Plant Matrix

Each ethanol extract was prepared from 5 g of ground/torn/trimmed/cut plant substrate in 50 mL of 96% ethanol (for UV VIS detection). The extraction time of organic matter lasted 1 h on a magnetic plate (400 rpm, 25 °C) in a dark, closed system due to the photoreduction of polyphenols [19].

#### 2.1.2. Water Extract of Plant Matrix

Collected plants and fruits were ground/torn/trimmed/cut and 5 g was added to 500 mL of distilled water in a boiling flask. Water extracts were prepared using the conventional decoction extraction method [20]. The plant material was slowly heated in a water bath to release its inner contents into a medium (at 70–80 °C, 2 h).

#### 2.1.3. Stock Solutions of Standards—GA and Q

Standard solutions consisted of GA (gallic acid, as a polyphenol representative) and Q (quercetin, as a flavonoid representative). Each solution was prepared in concentrations 0.1; 0.3; 0.5; 0.8; and 1.0 g.L<sup>-1</sup> in distilled water.

### 2.2. Determination of Total Polyphenol Content (TPC) in Selected Plants

The Folin–Ciocalteu method was used for polyphenol determination [21] with minor modifications. The absorbance was measured at 765 nm using a UV-1601 spectrophotometer (Shimadzu, Kyoto, Japan). The results were calculated using the calibration curve of the selected GA standard (1 g.L<sup>-1</sup>).

### 2.3. Green Synthesis of Fe-BNPs from Plants and Selected Standards

Prepared water extracts of the used plants were divided into 50 mL centrifugation tubes. The pH value was adjusted using 3M NaOH to 7–8 before iron salt was added (FeSO<sub>4</sub> · 7H<sub>2</sub>O) [22]. Green synthesis of Fe-BNPs was performed at laboratory temperature for 48 h on a reciprocal shaker (100 rpm) in the dark. Subsequently, synthesized Fe-BNPs were centrifuged twice (8000 rpm, 10 min) and immediately applied in the degradation experiments.

### 2.4. Setup Optimization Experiments for PCB Degradation by Synthetic nZVI

All the PCB degradation experiments were performed in 100 mL of distilled water (reagent flask) with the addition of Delor 103 (final concentration = 0.1 g.L<sup>-1</sup>) and nZVI (Nanofer 25S, NANO IRON s.r.o., Židlochovice, Czech Republic). Degradation took place on a rotary shaker (100 rpm) at 20 °C in the dark.

#### 2.4.1. Batch vs. Repeated Application of nZVI

In a single application, 2 g.L<sup>-1</sup> of nZVI (without pH adjustment) was added at the beginning and incubated for 28 days. The repeated application was performed by adding 0.5 g.L<sup>-1</sup> nZVI into the medium at regular time intervals (every 7th day) until a concentration of 2 g.L<sup>-1</sup> nZVI was reached.

#### 2.4.2. pH

The pH value in the reagent flask was adjusted to 10.1; 7.4; and 3.0 using 5% H<sub>2</sub>SO<sub>4</sub> and was measured over a period of 28 days.

### 2.4.3. Oxygen Requirements

The degradation of PCBs by nZVI ( $2 \text{ g.L}^{-1}$ ) was observed in the reagent flask (with limited oxygen access) and in Erlenmeyer flasks with cotton stoppers (with oxygen access) for 28 days.

## 2.5. Assessment of the PCB Degradation Efficiency

### 2.5.1. Degradation of PCBs by Synthesized Plant-Based Fe-BNPs

The reagent flask was filled with 100 mL of minimal mineral medium (MM medium) [23], a stock solution of Delor 103 ( $0.1 \text{ g.L}^{-1}$ ), and 3 mL of synthesized plant iron Fe-BNPs (or GA/Q iron bionanoparticles). The pH value was adjusted to 7–8 using 3 M NaOH. Flasks were then placed on a rotary shaker (100 rpm,  $20 \text{ }^\circ\text{C}$ ) for 7 days.

### 2.5.2. Degradation of PCBs by Individual Bacterial Strains

Bacterial strains were isolated from PCB-contaminated sediment from the Strážský canal. Adapted strains were able to persist and grow on the medium containing PCBs. The identification of bacteria was performed in our previous works using PCR methods [23] and confirmed using the MALDI-TOF method [24]. The Gram-negative strains *Ochrobactrum anthropi* (OA) and *Stenotrophomonas maltophilia* (SM) were used separately in the approach. The Erlenmeyer flask was filled with 100 mL of MM medium, a stock solution of Delor 103 ( $0.1 \text{ g.L}^{-1}$ ), and the bacterial inoculum ( $1 \text{ g.L}^{-1}$ ). The cultivation conditions were  $20 \text{ }^\circ\text{C}$  with stirring at 180 rpm for 14 days.

### 2.5.3. Sequential Approach—Nanobiodegradation of PCBs

The sequential approach to PCB degradation combined the use of Fe-BNPs for 7 days (in a reagent flask without oxygen access) and, subsequently, the addition of bacterial strain OA or SM (in an Erlenmeyer flask with a cotton stopper with oxygen access) for the next 14 days. The reagent flask was filled with 100 mL of MM media, a stock solution Delor 103 ( $0.1 \text{ g.L}^{-1}$ ), and 3 mL of synthesized plant Fe-BNPs (or GA/Q Fe-BNPs). After 7 days, the medium was poured into an Erlenmeyer flask, and the inoculum of the bacterial strain was added ( $1 \text{ g.L}^{-1}$ ). Experimental conditions were  $20 \text{ }^\circ\text{C}$  with stirring at 100 rpm (7 days) and 180 rpm (another 14 days).

## 2.6. Evaluation of PCB Degradation

The non-degraded PCBs were extracted by two-step n-hexane extraction ( $2 \times 10 \text{ mL}$  of n-hexane) [25]. Samples were analyzed using GC-ECD (HP 5890) in software ChemStation 4.0 (Agilent, Santa Clara, CA, USA). According to the prepared calibration of the standard mixture of the monitored PCB (six indicator congeners PCB 28, 52, 101, 118, 138, 153 and one selected PCB 8), the evaluation involved determining the percentage decrease of individual PCB congener based on the areas of their peaks.

## 3. Results and Discussion

### 3.1. Green Synthesis of Fe-BNPs from Plants and Selected Standards

Polyphenols are produced in every plant, fruit, or seed as secondary metabolites as a protective response to stressful conditions. In the experiment, 14 different parts of plants and fruits were analyzed to obtain basic knowledge about their bioactive compound contents. The interaction between these compounds and iron salt plays a key role in the green synthesis of Fe-BNPs. Therefore, it was important to determine the total content of phytochemicals in the used matrices. Plants are extremely complex materials with high contents of proteins, enzymes, lipids, or saccharides. The Folin–Ciocalteu method [21] provides an approximate estimate of total polyphenolic content, where other substances with an OH- group can also interact with the wolfram reagent. Consequently, the results may include other bioactive compounds present in the sample, potentially leading to a higher content. Nevertheless, the primary focus was on polyphenols and their interactions with iron salt to form Fe-BNPs for environmental (remediation) application. The chemical

interaction between major bioactive components could create a wide range of different Fe-BNPs and form an octahedral network with iron [12]. The most important requirement for the compounds to interact is to act as a carrier of the OH- group [9]; therefore, obtaining pure Fe-BNPs is challenging. Based on the results of the total polyphenol content (Table 1) in the selected plant substrates, seven with the highest polyphenol contents were further investigated for the green synthesis of Fe-BNPs.

**Table 1.** The total content of polyphenols (TPC) in used plant matrices.

| Plant/Fruit                              | Part        | TPC (mg GA.g <sup>-1</sup> ) | TPC from References (mg GA.g <sup>-1</sup> ) | References |
|------------------------------------------|-------------|------------------------------|----------------------------------------------|------------|
| Ivy ( <i>Hedera helix</i> )              | leaves      | 1.40                         | 1.50                                         | [26]       |
| Rosemary ( <i>Salvia rosmarinum</i> )    | leaves      | 3.80                         | 4.99                                         | [27]       |
| Pine ( <i>Pinus sylvestris</i> )         | needles     | 1.60                         | -                                            | -          |
| Sage ( <i>Salvia officinalis</i> )       | leaves      | 7.30                         | 31.25                                        | [28]       |
| Tangerine ( <i>Citrus reticulata</i> )   | peel        | 3.90                         | 3.83                                         | [29]       |
| Banana ( <i>Musa acuminata</i> )         | peel        | 2.20                         | 0.75                                         | [30]       |
| Melissa ( <i>Mellisa officinallis</i> )  | leaves      | 3.40                         | 51.00                                        | [31]       |
| Nettle ( <i>Urtica dioica</i> )          | leaves      | 0.39                         | 5.80                                         | [32]       |
| Orange ( <i>Citrus sineusis</i> )        | peel        | 1.80                         | 11.5                                         | [33]       |
| Magnolia ( <i>Magnolia grandiflora</i> ) | leaves      | 1.31                         | 14.3                                         | [34]       |
| Dill ( <i>Anethum graveoleus</i> )       | leaves      | 1.35                         | 1.51                                         | [35]       |
| Green tea ( <i>Camellia sinensis</i> )   | dry leaves  | 3.80                         | 3.07                                         | [36]       |
| Red grape Merlot                         | grape berry | 8.87                         | 2.02                                         | [37]       |
| Red grape Frankovka                      | grape berry | 10.27                        | 11.07                                        | [38]       |

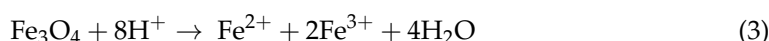
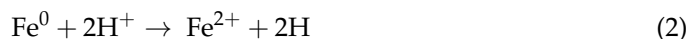
The primary and quickest method for observing iron bionanoparticle synthesis is the immediate change in color of the plant extract to dark brown or black [11]. The second and more detailed characterization involves the use of advanced devices such as Mössbauer spectroscopy, TEM, SEM, FT-IR, XRD, or Raman spectroscopy [13]. Material characterization using these techniques was not the subject of the current study. Instead, this study centers on the application of Fe-BNPs and verifies whether this is an effective degradation approach. The substrates chosen for the further experiments were rosemary, sage, banana, melissa, magnolia, and green tea.

Green synthesis of Fe-BNPs from the six selected plants was observed immediately after adding iron salt to the plant water extract, resulting in a color change. The quantity and properties of synthesized nanoparticles are greatly influenced by reaction conditions and the properties of the extract itself (pH value, reduction capacity, temperature, and extraction time) [39]. A previous study suggests that to extract almost all antioxidants, the extraction conditions should be at a maximum of 80 °C for 20 min in a solvent ratio of 1:1 (water:ethanol) using dried substrate [40]. The extraction yield may decrease if the extraction contact time exceeds 60–80 min, which depends on the part and type of fruit used, as flavins and catechol may degrade [41]. This degradation may be caused by factors related to the transfer of compounds from solid leaves to the aqueous phase, i.e., internal resistance [42]. The standard polyphenol and flavonoid representatives, GA and Q, were also tested in green synthesis to approximate the lowest or highest concentration of these compounds required to synthesize Fe-BNPs. After the synthesis, they were utilized in the subsequent set of experiments, i.e., for the degradation of PCBs.

### 3.2. Setup Optimization Experiments for PCB Degradation Process by Synthetic nZVI

The reactivity of nanoparticles is influenced by several factors, such as the presence of oxygen, salt ions, pH, and the concentration of nZVI itself. Among these factors, the effect of exposure to air oxygen, the initial pH, and, additionally, the impact of batch and repeated addition of nZVI were examined. Stable synthetic iron nanoparticles (Nanofer 25S, NANO IRON s.r.o., Židlochovice, Czech Republic) were used in the optimization setup experiment as standard due to their determined characteristics and properties. It is likely that there is a similar mechanism of action on harmful contaminants in nZVI and green synthesized bionanoparticles. The pH value plays an important role not only

in the preparation of nanoparticles, affecting their morphology (size and shape), but also significantly influences their reactivity in the degradation process [6]. The prepared reaction mixture was exposed to initial pH values of 10 (unchanged, original), 7, and 3 in distilled water with the addition of nZVI particles and Delor 103 (PCB congeners commercial mixture) for 28 days. The results for each initial pH value show that the highest degradation rate was achieved at pH 3, where the percentage of degradation summed by all the monitored PCB congeners accounted for 39%. The degradation rates at pH 7 and at pH 10 were slightly lower (37% and 35%, respectively). Although the data do not show a notable difference, they indicate a possible correlation; a decrease in pH might enhance the degradation rate of chlorinated pollutants. The reason for this could be attributed to an acidic environment, where the reactivity of nanoparticles is enhanced by accelerating iron corrosion and dissolving the passivating layer on the nZVI surface. Conversely, in an alkaline environment, there is a decrease in reactivity due to the precipitation of iron hydroxides on the nanoparticles' surfaces, resulting in the inhibition of electron transfer from the Fe<sup>0</sup> nucleus to the uppermost layer [43]. A previous study recorded similar findings in PCB nanoremediation of contaminated soil [6]. The results of that study indicate that an environment with a pH value below 5 does not noticeably affect degradation efficiency. This is because, at the indicated pH value, a sufficient number of protons capable of accelerating PCB dechlorination are generated. In our study, the presence of H<sub>2</sub>SO<sub>4</sub> negatively affected the interaction of iron nanoparticles with PCBs. This is supported by other studies that show that lowering the pH below 3.8 initiates a decrease in the reactivity of iron due to its rapid loss via the dissolution process. Previous work further shows that degradation is inhibited by the presence of anions (HPO<sub>4</sub><sup>2-</sup>, HCO<sub>3</sub><sup>-</sup>, SO<sub>4</sub><sup>2-</sup> and Cl<sup>-</sup>) due to the formation of complexes with iron oxides on the surface of nZVI [43]. Additionally, the change in pH value was periodically monitored for 14 days from the start with initial values of pH 3, 7, and 10. After this time, the pH of each solution settled at near neutral values. The solutions with an initial pH value of 3, 7, and 10 had pH values of 6, 5, 8, and 9, respectively, after exposure to nZVI for 14 days. The significant increase in pH in the initially acidic solution was probably induced by the consumption of hydrogen ions via two possible reaction mechanisms ((2) and (3)) [44]:



The subsequent decrease in the pH of the more alkaline mixtures may have been caused by the adsorption of the contaminant to the completely oxidized nanoparticle surface [42]. Neutralization of solutions could have also led to the formation of agglomerates [45]. At pH 7, smaller particles exhibit a lower charge compared to larger particles. This results in diminished electrical double layer (EDL) repulsion forces, consequently increasing the tendency for aggregation. Particles smaller than 100 nm are inherently highly reactive, capable of interacting not only with contaminants but also with each other, leading to either hetero- or homo-aggregation. As a result, there is a consistent likelihood that these nanoparticles could form larger structures, such as microparticles, through agglomeration, subsequently reducing their reactivity [45,46]. Interestingly, after 28 days of degradation with different pH values, a slight change in color was observed in each case. In a mixture with an initial pH of 7, H<sub>2</sub>SO<sub>4</sub> is presumed to dissolve the oxide layer, forming iron ions with a predominant Fe<sup>3+</sup> abundance. This process generates FeOOH (rusty color) in the aquatic environment. In a more acidic environment (pH 3), there is massive dissolution of the Fe<sup>0</sup> nucleus itself, releasing Fe<sup>2+</sup> ions that interact with water to form Fe(OH)<sub>2</sub> (green color).

The effect of oxygen on the degradation capability of nZVI was tested in reagent flasks with closed tops and in Erlenmeyer flasks with cotton stoppers, allowing potential oxygen penetration. Avoiding oxygen access is key to achieving enhanced degradation. The degradation of PCBs by nZVI with access to air oxygen was minimal (4%). Conversely,

in a reagent flask without access to air oxygen, the degradation reached 65%. This indicates the importance of preventing air oxygen from entering the system. It is known that the remediation of halogenated pollutants mostly involves the process of reducing dehalogenation, wherein the oxidation of nZVI to  $\text{Fe}^{2+}$  ions generate the necessary electrons for dechlorination. Under anaerobic conditions, the electrons, as products of the reaction of nZVI with water, are involved in the reduction of the chlorinated compound. However, under aerobic conditions, oxygen acts as the preferred electron acceptor [47]. The surface of the  $\text{Fe}^0$  core is coated with a compact layer of iron oxides dominated by  $\text{Fe}^{3+}$  ions (with an observed rusty coloration of the mixture in the Erlenmeyer flasks). This coating partially prevents the degradation of chlorinated pollutants. The process in which nanoparticles are exposed to air oxygen and oxidized is referred to as “aging” [44].

The effectiveness of the batch application of nZVI ( $2 \text{ g.L}^{-1}$ ) vs. repeated application (each  $0.5 \text{ g.L}^{-1}$  until reaching  $2 \text{ g.L}^{-1}$ ) on the degradation of PCBs was also assessed. The results indicate that the repeated application of nZVI is more beneficial as the overall degradation efficiency reached 80%, whereas for a batch application, this was only 57%. The explanation for these results may lie in the tendency of nanoparticles to cluster together and form agglomerates. Aggregation reduces the specific surface area of nZVI available for interaction with pollutants [16]. When nanoparticles are applied in smaller quantities, the probability of forming such formations is lower, as they are more dispersed in the environment. Additionally, with repeated doses of “fresh” nanoparticles, the degradation process is prolonged. This elongation occurs because, with time, the reactivity of nZVI also decreases due to the formation of a solid passivating layer.

### 3.3. Degradation of PCBs

#### 3.3.1. Degradation of PCBs by Synthesized Plant-Based Fe-BNPs

After the green synthesis of Fe-BNPs from six different substrates, the degradation of PCBs was performed. Initially, the newly synthesized Fe-BNPs were applied for the degradation of the PCB mixture Delor 103 in an artificially contaminated MM medium for 7 days. Figure 1 describes the percentages of degradation of the selected individual PCB congeners and the sum of seven PCB congeners using Fe-BNPs synthesized from the selected plants and fruits.

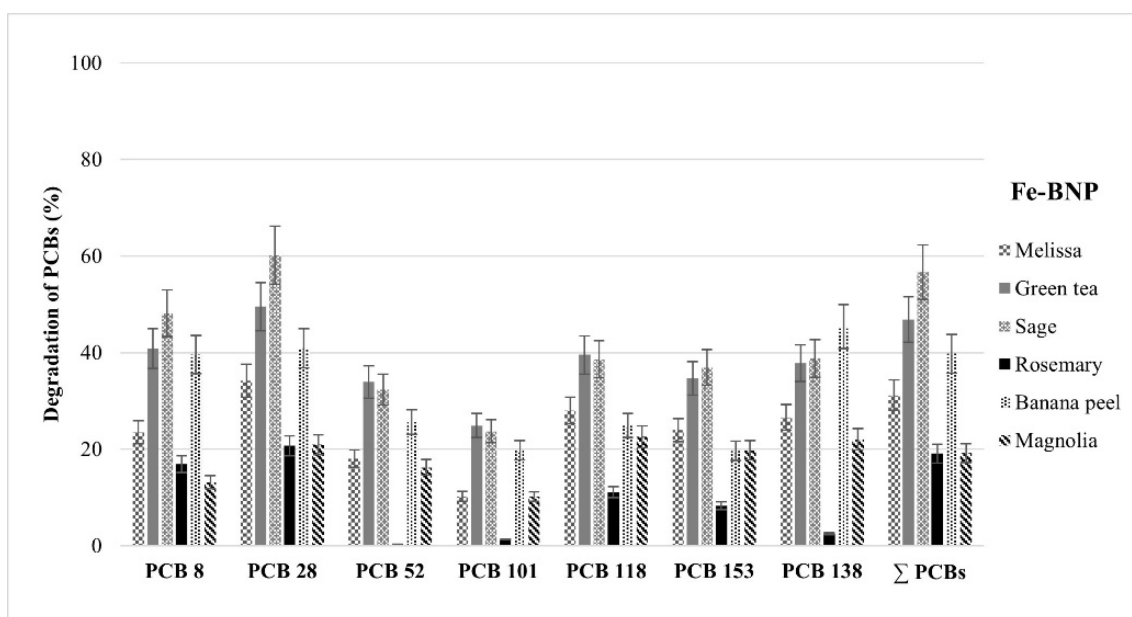


**Figure 1.** Degradation of PCBs using Fe-BNPs synthesized from six different substrates. Experimental conditions: 7 days, 20 °C, and 100 rpm.

The results show that Fe-BNPs derived from sage achieved the highest total degradation of the seven PCB congeners (56%). The next most effective Fe-BNPs were those derived from green tea and banana peel. Additionally, Fe-BNPs from sage achieved a degradation of up to 60% for the individual congener PCB 28. A previous study observed a similar percentage reduction in the sum of PCB 28 and 52 (as the most abundant PCB congeners in the mixture Delor 103) using micro-scale zero-valent iron (72.2%) and synthetic nanoparticles (81.3%) in artificially contaminated water [48]. Fe-BNPs from melissa, rosemary, and magnolia had lower attained effectiveness. The main reason for this could be an insufficient number of OH- groups in their water extracts, which iron could not chelate. This would lead to a lower Fe-BNPs yield (not determined), and, thus, lower degradation activity. As previously mentioned, it is also crucial to set optimal experimental conditions to achieve the highest possible content of bioactive substances in the extract. A potentially higher degradation effect could be achieved by completely restricting the access of air oxygen (to prevent the passivation of Fe-BNPs) and replacing it with an inert atmosphere with nitrogen. However, this would limit the usability in situ. Plant nanoparticles have great potential for decontaminating a wide range of pollutants from the environment. Nanoparticles synthesized from green tea effectively removed 59.7% of nitrates from the water environment [49]. Magnolia-derived Fe-BNPs even managed to eliminate up to 98.84% of phosphates present in wastewater [50]. Green tea nanoparticles were also prepared in another work and applied to the reduction of Cr<sup>6+</sup> cations in an aqueous environment [51]. These nanoparticles exhibited a reduction capacity as high as 500 mg Cr (VI) per g of iron in nanoparticles. Polyphenol (GA) and flavonoid (Q) representatives were also tested in the synthesis of Fe-BNPs and subsequently used for the degradation of the sum of PCB congeners at five different concentrations. It can be concluded that the same concentrations of GA and Q during the formation of Fe-BNPs do not necessarily lead to the same degradation ability (Figure 2). Fe-BNPs from GA achieved the highest percentage of Delor 103 degradation at a concentration of 0.1 g.L<sup>-1</sup>, which was up to 73%.

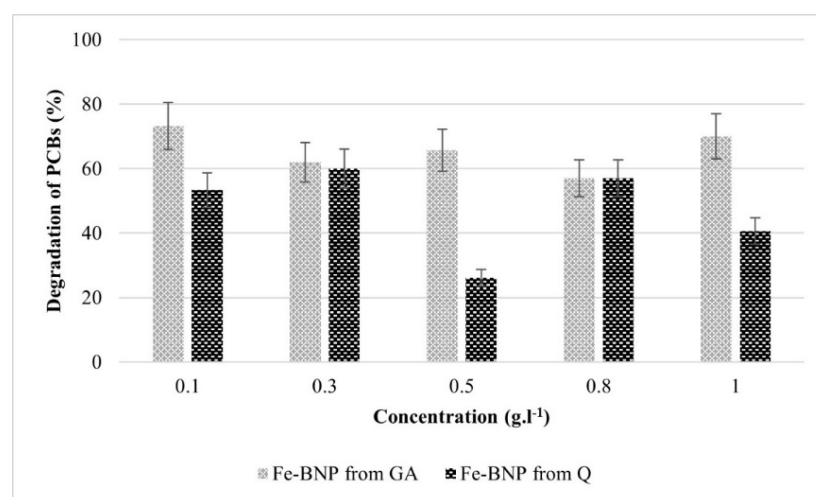


**Figure 2.** Degradation of the sum of seven PCB congeners using iron bionanoparticles from Q (Q-derived Fe-BNPs) and iron bionanoparticles from GA (GA-derived Fe-BNPs) at five different concentrations (0.1; 0.3; 0.5; 0.8; and 1 g.L<sup>-1</sup>). Experimental conditions: 7 days, 20 °C, and 100 rpm.

Slightly lower values were measured at concentrations of 0.5 g.L<sup>-1</sup> and 1 g.L<sup>-1</sup>. The percentage degradation at 0.3 g.L<sup>-1</sup> and 0.8 g.L<sup>-1</sup> was around 60%. GA-derived Fe-BNPs had a higher degradation effect than Q-derived Fe-BNPs. Fe-BNPs synthesized from Q achieved the highest percentage degradation (60%) at a concentration of 0.3 g.L<sup>-1</sup>. The degradation percentage was comparable at the concentration of 0.1 g.L<sup>-1</sup>. However, at 1 g.L<sup>-1</sup>, a value of 40% was recorded, while the lowest percentage degradation was measured at 0.5 g.L<sup>-1</sup>. This study aimed to determine the optimal concentrations of

polyphenols and flavonoids (using gallic acid (GA) and quercetin (Q) as model compounds representing bioactive substances in plant substrates) for precipitating with an iron precursor into bionanoparticles (Fe-BNPs) and, thereby, observing their effect on PCB degradation. By identifying the concentrations of GA and Q that result in the maximum formation of Fe-BNPs and the most effective PCB degradation, the yield and degradation efficacy of Fe-BNPs synthesized from substrates with known bioactive substance concentrations can be more accurately predicted. This also allows for methodological adjustments to achieve the highest possible degradation rates. This study indicates that polyphenols (GA) act as the main agents in the reaction, forming bionanoparticles capable of degrading PCBs even at low concentrations. In contrast, increasing the concentration of flavonoids (Q) used for bionanoparticle preparation did not result in higher PCB degradation.

These results suggest that each phenolic compound creates different structures and shapes of nanoparticles and, therefore, react differently. Since the reducing ability of Fe-BNPs is directly influenced by their shape and size, the specific compound can contribute to defining their final effect on the degradation of individual PCB congeners [52]. By comparing the degradation results of PCBs obtained from plant-based Fe-BNPs and Fe-BNPs derived from phenolic standards (GA and Q), optimal concentrations of polyphenols and flavonoids for Fe-BNPs preparation were indicated. For example, an extract prepared from sage contained  $0.73 \text{ g.L}^{-1}$  of polyphenols. Following the synthesis of Fe-BNPs, a PCB degradation rate of 56% was achieved. Fe-BNPs derived from GA at concentrations ranging  $0.5\text{--}0.8 \text{ g.L}^{-1}$  achieved a degradation rate of 56–65% for the sum of seven PCB congeners, which is comparable with the degradation effectiveness of the Fe-BNPs from sage. The concentrations of polyphenols and flavonoids in green tea extract were  $0.38 \text{ g.L}^{-1}$  and  $0.08 \text{ g.L}^{-1}$ , respectively. The water extract of melissa contained  $0.34 \text{ g.L}^{-1}$  of polyphenols and  $0.24 \text{ g.L}^{-1}$  of flavonoids. The percentages of nanodegradation at these concentrations were 46% and 31% for green-tea-derived Fe-BNPs and melissa-derived Fe-BNPs, respectively. When comparing these results for flavonoids, it is evident that lower concentrations of  $0.1 \text{ g.L}^{-1}$  and  $0.3 \text{ g.L}^{-1}$  are more efficient. This is also signified by the highest percentage degradation of PCBs at these concentrations. Polyphenols at a concentration of  $0.3 \text{ g.L}^{-1}$ , as roughly measured in the green tea and melissa extracts, showed minor degradation at all other concentrations. Degradation was only 7% lower with Fe-BNPs from green tea, while a decrease of up to 20% was seen using Fe-BNPs from melissa. According to the obtained results, it can be concluded that in the case of phenolic compounds, the degradation of PCBs by Fe-BNPs formed from these phenolic compounds does not depend only on their concentration but also on the representation of specific compounds, including flavonoids, phenols, stilbenes, tannins, and lignins [10]. Certainly, a challenging scenario can arise wherein some substances present in the matrix can inhibit the synthesis of Fe-BNPs from polyphenols. The presence of these components may result in a change in the pH or redox conditions in the prepared plant extract and thus prevent interactions between the iron salt and key polyphenols.

### 3.3.2. Degradation of PCBs by Individual Bacterial Strains

The bacterial strains used in this experiment were isolated from the contaminated site known as the “Strážsky canal”, which flows out of the Chemko Strážske plant. This location is notorious for its high contamination with PCB substances. The selected bacteria, *Ochrobactrum anthropi* (OA), and *Stenotrophomonas maltophilia* (SM), are both gram-negative aerobic strains, which were employed in our previous studies on the biodegradation of PCBs [24,53]. Both of the selected bacterial strains were capable of degrading PCBs to a similar extent, as illustrated in Figure 3, with approximately 62–63% degradation of the sum of seven PCB congeners.

These bacterial strains, isolated from the PCB-contaminated shallow creek sediment, typically utilize biphenyl (the non-chlorinated structural analogue of PCBs) as a carbon and energy source. Consequently, these strains possess the capacity to degrade PCBs via the biphenyl metabolic pathway [24]. Higher chlorinated PCBs are often less accessible to

bacteria due to their torsion angles. Consequently, the biodegradation of lower chlorinated congeners is more feasible and, therefore, more efficient [52]. However, this phenomenon was not observed in the present study. Only PCB 101 was degraded to a lesser extent compared to highly chlorinated congeners PCB 118, 153, and 138. Nevertheless, previous works have established that the bacterial strain OA can degrade various chlorinated PCB congeners regardless of the number of chlorines per molecule. Specifically, it was observed that OA was capable of biodegrading 68% of the sum of seven PCB congeners after 21 days [53]. In a previous study, the bacterial strains *S. maltophilia* and *O. anthropi* used for the biodegradation of PCBs showed degradation abilities of 40% and 60%, respectively [54]. These results indicate possible limitations of using individual isolated microorganisms for the degradation of various chlorinated PCB congeners.

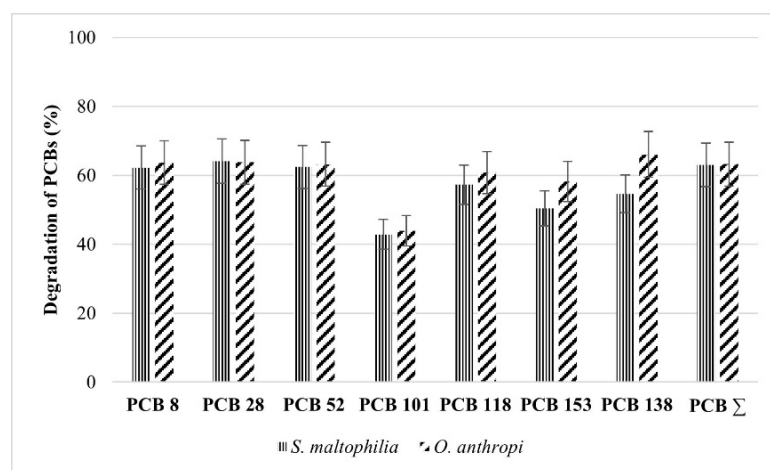


**Figure 3.** Degradation of PCBs by individual bacterial strains *Ochrobactrum anthropi* and *Stenotrophomonas maltophilia*. Experimental conditions: 14 days, 20 °C, and 180 rpm.

### 3.3.3. Sequential Approach—Nanobiodegradation of PCBs

The sequential approach combines abiotic and biotic conditions, aiming to increase PCB degradation. The theory behind this methodology is that Fe-BNPs dechlorinate or absorb higher chlorinated PCB congeners that are less accessible to bacteria. Subsequently, upon inoculation with bacterial strains, these lower chlorinated PCBs are degraded. The highest PCB degradation rate (75%) was achieved in the sequential approach starting with the addition of Fe-BNPs from sage followed by the addition of the bacterial strain SM (Figure 4). During the sequential degradation using the bacterial strain OA (Figure 5), approximately 50% PCB degradation was achieved, representing a decrease compared to the degradation solely using Fe-BNPs from sage (these Fe-BNPs alone achieved a degradation of 57% after 7 days, i.e., before the application of the bacterial strain).

Fe-BNPs from rosemary achieved the highest percentage degradation in the sequential degradation with the bacterial strain SM (45%). Following the addition of the bacterial strain OA, an increase in degradation was observed compared to the effect of Fe-BNPs alone (19%). The introduction of Fe-BNPs from green tea resulted in a decrease in PCB degradation upon the addition of both bacterial strains. This decline could be attributed to the potential antibacterial properties of the green tea extract [55]. In the sequential degradation using Fe-BNPs from melissa and both bacterial strains (applied in different sets of experiments), an increase in degradation was observed compared to nanodegradation by Fe-BNPs alone. The combination of abiotic and biotic treatments for the degradation of a solution containing Aroclor 1248 (PCBs) was previously studied [16] using nZVI (1000 mg.L<sup>-1</sup>) followed by the subsequent addition of *Burkholderia xenovorans*. This process resulted in 89% degradation of the sum of PCB congeners. A sequential reduction–oxidation method was also employed for complete degradation (100% achieved in only 10 h of exposure) of triclosan in aqueous solution. Under anaerobic conditions, Pd/nFe was used with a laccase coating derived from

*Trametes versicolor* in the presence of a redox mediator [56]. The nano-bio redox method, consisting of nZVI and an aerobic bacterium *Sphingomonas* sp. PH-07, demonstrated the effective degradation of polybrominated diphenyl ethers (PBDEs) to bromophenols and other metabolites following the addition of bacteria for 4 days [14].

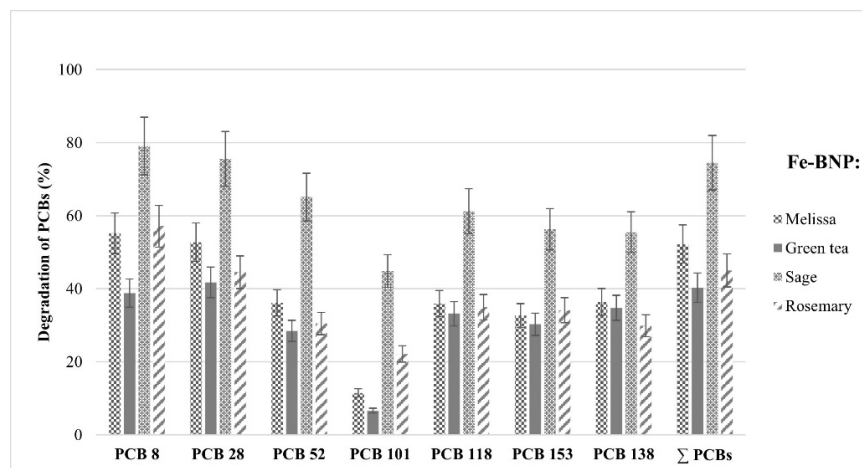


**Figure 4.** Sequential degradation of PCBs using plant-based Fe-BNPs and the bacteria *S. maltophilia*. Experimental conditions: 7-day cultivation with limited oxygen access to the reagent flask (3 mL of Fe-BNPs) at 25 °C and 100 rpm, and then 14-day cultivation under aerobic conditions (1 g.L<sup>-1</sup> of bacterial inoculum at 25 °C and 180 rpm).

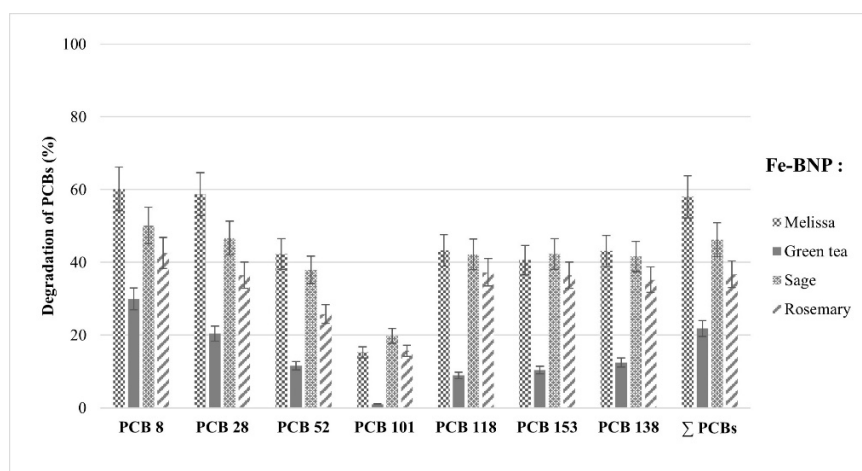


**Figure 5.** Sequential degradation of PCBs using plant-based Fe-BNPs and the bacteria *O. anthropi*. Experimental conditions: 7-day cultivation with limited oxygen access to the reagent flask (3 mL of Fe-BNPs) at 25 °C and 100 rpm, and then 14-day cultivation under aerobic conditions (1 g.L<sup>-1</sup> of bacterial inoculum) at 25 °C and 180 rpm.

According to Figure 6, the degradation ability of PCBs again differs when comparing the same concentrations of GA and Q for the formation of Fe-BNPs. The most effective concentrations of polyphenols for Fe-BNP synthesis during the sequential approach were 0.5 g.L<sup>-1</sup> and 0.8 g.L<sup>-1</sup>, resulting in PCB degradation up to 90%. This was the highest achieved result in the experiment. For comparison, the Fe-BNPs from sage (with a GA content of 0.73 g.L<sup>-1</sup>) had approximately the same degradation effects as nanobiodegradation with the SM bacterial strain. The lowest degradation was recorded at a concentration of 0.1 g.L<sup>-1</sup>. Conversely, when using Fe-BNPs from flavonoids, the percentage of degraded PCBs decreased as the concentration increased.

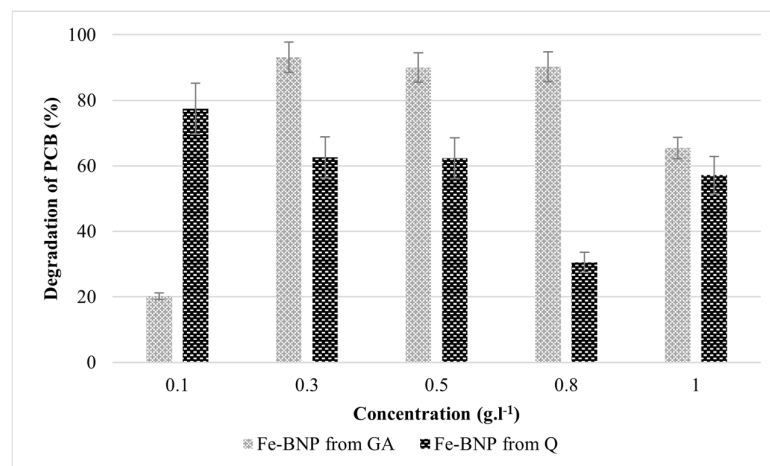


**Figure 6.** Sequential degradation of the sum of PCB congeners using Fe-BNPs from GA and Fe-BNPs from Q with the addition of bacterial strain *O. anthropi* (OA). Experimental conditions: 7-day anaerobic cultivation at 25 °C and 100 rpm, and then 14-day aerobic cultivation and 25 °C and 180 rpm.

Through this experiment using individual selected standards of polyphenols and flavonoids, recognized as key components for the synthesis of Fe-BNPs in literature [11,13], the minimum necessary amount for Fe-BNP formation and their PCB-degrading ability were roughly estimated. Among the selected concentrations of pure standards, the optimal concentration (in the nanobiodegradation method) for polyphenols (GA) was found to be in the range of 0.3–0.8 g.L<sup>-1</sup>. Conversely, for flavonoids, a lower concentration of 0.1 g.L<sup>-1</sup> proved to be more effective. When comparing the results obtained from the nanodegradation of Fe-BNPs alone versus the nanobiodegradation, the sequential approach appears to be more effective for PCB decontamination, which is also indicated by Figure 7. Fe-BNPs from melissa, sage, and rosemary in combination with the addition of bacterial strains (OA or SM) attained higher degradation results when compared to their individual use in the degradation of PCBs.

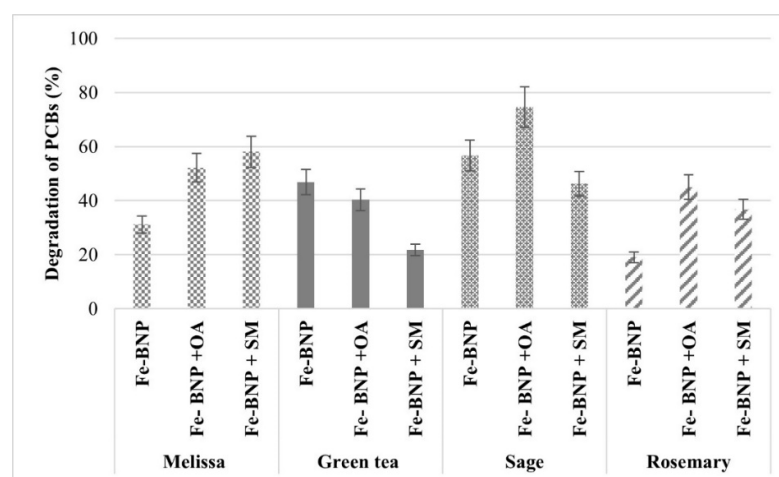


**Figure 7.** Graphical comparison of nanodegradation (Fe-BNPs applied individually) and nanobiodegradation of PCBs (Fe-BNPs with subsequent application of bacterial strain OA or SM) approaches with four different Fe-BNPs prepared from selected plants.

Nanobioremediation involves the use of nanoparticles to reduce the higher chlorination of contaminants to lower chlorinated compounds that are more accessible to biodegradation [14]. Subsequently, this process promotes the biodegradation of the contaminants into harmless products. The integration of green synthesis from plants, food, or

food waste (which aligns with a circular economy) to create Fe-BNPs, is an effective and sustainable approach for remediating numerous contaminated sites worldwide. Further studies and developmental efforts are required to facilitate the widespread implementation of this technology at full scale.

#### 4. Conclusions

The green synthesis of Fe-BNPs from selected plants and fruits offers a novel approach for PCB removal. Fe-BNPs were successfully synthesized from sage, banana, green tea, magnolia, rosemary, and melissa. Selected concentrations of pure standards of polyphenols and flavonoids revealed an approximate range for Fe-BNPs synthesis. Both bacterial strains proved to have a similar PCB-degrading efficiency (62–63%). The sequential application of Fe-BNPs, and the subsequent addition of the bacterial strains, demonstrated the most promising results among the performed experiments. The addition of sage-derived Fe-BNPs with the bacteria *Stenotrophomonas maltophilia* achieved the highest degradation rate among the used degradation approaches from plant bionanoparticles (75%). The optimal concentration for the green synthesis of bionanoparticles aimed at PCB degradation was found to be between 0.3 and 0.8 g.L<sup>-1</sup> of gallic acid in conjunction with the bacterial strain *Ochrobactrum anthropi* (92% degradation of PCBs). This study presents a novel approach, whereby Fe-BNPs generated by green synthesis were combined sequentially with bacteria possessing the necessary degradation capabilities to optimize PCB degradation.

**Author Contributions:** Conceptualization, M.T., H.H. and K.D.; methodology, M.T., H.H. and K.D.; validation, M.T. and H.H.; formal analysis, M.T.; investigation, M.T., M.M., M.H. and K.T.; resources, L.J.; writing—original draft preparation, M.T.; writing—review and editing, H.H., K.D. and M.M.; visualization, M.M., M.H. and K.T.; project administration, H.H., M.T. and K.D.; funding acquisition, L.J. All authors have read and agreed to the published version of the manuscript.

**Funding:** This research was financially supported by student grant from Comenius University UK/168/2023 and UK/3039/2024 and funded by the European Union under the Horizon Europe project (RIA), project number 101112723—Achieving remediation and governing restoration of contaminated soils now (ARAGORN). The expressed opinions and views are those of the authors and do not necessarily reflect the requirements of the European Union. The European Union is not responsible for them. This work was also supported by the Slovak Research and Development Agency under contract No. APVV-0656-12 and by the Scientific Grant Agency of the Ministry of Education, Science, and Sport of the Slovak Republic (Grant No. 1/0295/15).

**Data Availability Statement:** The original contributions presented in the study are included in the article, and further inquiries can be directed to the corresponding author.

**Acknowledgments:** I sincerely thank my colleagues for their unwavering support and patience during the writing of this research paper. Your insightful feedback and encouragement were invaluable. I am grateful for your understanding and collaboration throughout this process. Thank you for your constant support.

**Conflicts of Interest:** Author Hana Horváthová was employed by the Centre of Environmental Services, Ltd. The remaining authors declare that the research was conducted in the absence of any commercial or financial relationships that could be construed as a potential conflict of interest. The Centre of Environmental Services, Ltd. had no role in the design of the study; in the collection, analyses, or interpretation of data; in the writing of the manuscript, or in the decision to publish the results.

#### References

1. Kočan, A.; Petrik, J.; Jursa, S.; Chovancova, J.; Drobna, B. Environmental contamination with polychlorinated biphenyls in the area of their former manufacture in Slovakia. *Chemosphere* **2001**, *43*, 595–600. [[CrossRef](#)] [[PubMed](#)]
2. Xie, M.; Xu, L.; Zhang, R.; Zhou, Y.; Xiao, Y.; Su, X.; Shen, C.; Sun, F.; Hashmi, M.Z.; Lin, H.; et al. Viable but Nonculturable State of Yeast *Candida* sp. Strain LN1 Induced by High Phenol Concentrations. *Environ. Microbiol.* **2021**, *87*, e01110-21. [[CrossRef](#)] [[PubMed](#)]
3. Khalid, F.; Hashmi, M.Z.; Jamil, N.; Qadir, A.; Ali, M.I. Microbial and enzymatic degradation of PCBs from e-waste-contaminated sites: A review. *Environ. Sci. Pollut. Res.* **2021**, *28*, 10474–10478. [[CrossRef](#)] [[PubMed](#)]

4. Akhondi, M.; Dadkhah, A.A. Base-catalysed decomposition of polychlorinated biphenyls in transformer oils by mixture of sodium hydroxide, glycerol and iron. *R. Soc. Open Sci.* **2018**, *5*, 172401. [[CrossRef](#)] [[PubMed](#)]
5. Taka, A.L.; Tata, C.M.; Klink, M.J.; Mbianda, X.Y.; Mtunzi, F.M.; Naidoo, E.B. A Review on Conventional and Advanced Methods for Nanotoxicology Evaluation of Engineered Nanomaterials. *Molecules* **2021**, *26*, 6536. [[CrossRef](#)] [[PubMed](#)]
6. Zhang, H.; Zhang, B.; Liu, B. Integrated Nanozero Valent Iron and Biosurfactant-Aided Remediation of PCB-Contaminated Soil. *Appl. Environ. Soil Sci.* **2016**, *2016*, 5390808. [[CrossRef](#)]
7. Iqbal, P.; Preece, J.A.; Mendes, P.M. Nanotechnology: The “Top-Down” and “Bottom-Up” Approaches. In *Supramolecular Chemistry*; Gale, A.P., Ed.; Wiley: Hoboken, NJ, USA, 2012; ISBN 9780470661345. [[CrossRef](#)]
8. Dikshit, P.K.; Kumar, J.; Das, A.K.; Sadhu, S.; Sharma, S.; Singh, S.; Gupta, P.K.; Kim, B.S. Green Synthesis of Metallic Nanoparticles: Applications and Limitations. *Catalysts* **2021**, *11*, 902. [[CrossRef](#)]
9. Pal, G.; Rai, P.; Pandey, A. Chapter 1-Green synthesis of nanoparticles: A greener approach for a cleaner future. In *Green Synthesis, Characterization and Applications of Nanoparticles*; Shukla, A.K., Irvani, S., Eds.; Elsevier: Amsterdam, The Netherlands, 2019; pp. 1–26. ISBN 978-0-08-102579-6. [[CrossRef](#)]
10. Tijjani, H.; Zangoma, M.H.; Mohammed, Z.S.; Obidola, S.M.; Egbuna, C.; Abdulai, S.I. Polyphenols: Classifications, Biosynthesis and Bioactivities. In *Functional Foods and Nutraceuticals*; Egbuna, C., Dable Tupas, G., Eds.; Springer: Berlin/Heidelberg, Germany, 2020; pp. 389–414. ISBN 978-3-030-42319-3. [[CrossRef](#)]
11. Sunardi, A.; Rahardjo, S.B.; Environ, I.-J. Green Synthesis and Characterization of nano Zero Valent Iron Using Banana Peel Extract. *J. Environ. Earth Sci.* **2017**, *7*, 80–84.
12. Kasprzak, M.M.; Erxleben, A.; Ochocki, J. Properties and applications of flavonoid metal complexes. *RSC Adv.* **2015**, *5*, 45853–45877. [[CrossRef](#)]
13. Markova, Z.; Novak, P.; Kaslik, J.; Plachtova, P.; Brazdova, M.; Jancula, D.; Siskova, K.M.; Machala, L.; Marsalek, B.; Zboril, R.; et al. Iron(II,III)-Polyphenol Complex Nanoparticles Derived from Green Tea with Remarkable Ecotoxicological Impact. *ACS Sustain. Chem. Eng.* **2014**, *2*, 1674–1680. [[CrossRef](#)]
14. Singh, R.; Behera, M.; Kumar, S. Nano-bioremediation: An Innovative Remediation Technology for Treatment and Management of Contaminated Sites. In *Bioremediation of Industrial Waste for Environmental Safety: Volume II: Biological Agents and Methods for Industrial Waste Management*; Bharagava, R.N., Saxena, G., Eds.; Springer: Berlin/Heidelberg, Germany, 2020; pp. 165–182. [[CrossRef](#)]
15. Cecchin, I.; Reddy, K.R.; Thomé, A.; Tessaro, E.F.; Schnaid, F. Nanobioremediation: Integration of nanoparticles and bioremediation for sustainable remediation of chlorinated organic contaminants in soils. *Int. Biodeterior. Biodegrad.* **2017**, *119*, 419–428. [[CrossRef](#)]
16. Le, T.T.; Nguyen, K.-H.; Jeon, J.-R.; Francis, A.J.; Chang, Y.-S. Nano/bio treatment of polychlorinated biphenyls with evaluation of comparative toxicity. *J. Hazard. Mater.* **2015**, *287*, 335–341. [[CrossRef](#)] [[PubMed](#)]
17. Yadav, K.; Singh, J.; Gupta, N.; Kumar, V. A Review of Nanobioremediation Technologies for Environmental Cleanup: A Novel Biological Approach. *J. Mater. Environ. Sci.* **2017**, *8*, 740–757.
18. Gomes, H.I.; Ottosen, L.M.; Ribeiro, A.B.; Dias-Ferreira, C. Treatment of a suspension of PCB contaminated soil using iron nanoparticles and electric current. *J. Environ. Manag.* **2015**, *151*, 550–555. [[CrossRef](#)] [[PubMed](#)]
19. Alara, O.; Abdurahman, N.; Olalere, O. Ethanol extraction of flavonoids, phenolics and antioxidants from Vernonia amygdalina leaf using two-level factorial design. *J. King Saud Univ. Sci.* **2020**, *32*, 7–16. [[CrossRef](#)]
20. Hidayat, R.; Wulandari, P. Methods of Extraction: Maceration, Percolation and Decoction. *Eureka Herba Indones.* **2021**, *2*, 73–79. [[CrossRef](#)]
21. Lamuela-Raventós, R.M. Folin-Ciocalteu method for the measurement of total phenolic content and antioxidant capacity. In *Measurement of Antioxidant Activity & Capacity*; Apak, R., Capanoglu, E., Shahidi, F., Eds.; Wiley: Hoboken, NJ, USA, 2018; pp. 107–115. ISBN 9781119135388. [[CrossRef](#)]
22. Solmošiová, M.; Hrdlička, L.; Prousek, J. Preparation of nanoscale zero-valent iron by reduction of ferrous sulfate with the use of magnolia leaves extracts and its application for degradation of coloured solutions by Fenton-like reaction. In Proceedings of the Aplikované Prírodné Vedy, Trnava, Slovakia, 6 April 2016; pp. 47–51. (In Slovak).
23. Dudášová, H.; Lukáčová, L.; Murínová, S.; Puškárová, A.; Pangallo, D.; Dercová, K. Bacterial strains isolated from PCB-contaminated sediments and their use for bioaugmentation strategy in microcosms. *J. Basic Microbiol.* **2013**, *54*, 253–260. [[CrossRef](#)] [[PubMed](#)]
24. Lászlová, K.; Dudášová, H.; Olejníková, P.; Horváthová, G.; Velická, Z.; Horváthová, H.; Dercová, K. The Application of Biosurfactants in Bioremediation of the Aged Sediment Contaminated with Polychlorinated Biphenyls. *Water Air Soil Pollut.* **2018**, *229*, 219. [[CrossRef](#)]
25. Dudášová, H.; Lukáčová, L.; Murínová, S.; Dercová, K. Effects of plant terpenes on biodegradation of polychlorinated biphenyls (PCBs). *Int. Biodeterior. Biodegrad.* **2012**, *69*, 23–27. [[CrossRef](#)]
26. Pop, C.; Pârvu, M.; Arsene, A.; Pârvu, A.E.; Vodnar, D.; Tarcea, M.; Toiu, A.; Vlase, L. Investigation of antioxidant and antimicrobial potential of some extracts from *Hedera helix* L. *Farmacía* **2017**, *65*, 624–629.
27. Tavassoli, S.; Djomeh, Z.E. Total phenols, antioxidant potential and antimicrobial activity of methanol extract of rosemary (*Rosmarinus officinalis* L.). *Glob. Vet.* **2011**, *7*, 337–341.
28. Abdelkader, M.; Ahcen, B.; Rachid, D.; Hakim, H. Phytochemical Study and Biological Activity of Sage (*Salvia officinalis* L.). *World Acad. Sci. Eng. Technol. Int. J. Biol. Biomol. Agric. Food Biotechnol. Eng.* **2015**, *8*, 1253–1257.

29. Damián-Reyna, A.A.; González-Hernández, J.C.; Maya-Yescas, R.; de Jesús Cortés-Penagos, C.; del Carmen Chávez-Parga, M. Polyphenolic content and bactericidal effect of Mexican *Citrus limetta* and *Citrus reticulata*. *J. Food Sci. Technol.* **2017**, *54*, 531–537. [[CrossRef](#)] [[PubMed](#)]
30. Fatameh, S.R.; Saifullah, R.; Abbas, F.M.A.; Azhar, M.E. Total phenolics, flavonoids and antioxidant activity of banana pulp and peel flours: Influence of variety and stage of ripeness. *Int. Food Res. J.* **2012**, *19*, 1041–1046.
31. Behbahani, B.A.; Shahidi, F. *Melissa officinalis* Essential Oil: Chemical Compositions, Antioxidant Potential, Total Phenolic Content and Antimicrobial Activity. *Nutr. Food Sci. Res.* **2019**, *6*, 17–25. [[CrossRef](#)]
32. Kőszegi, K.; Békássy-Molnár, E.; Koczka, N.; Kerner, T.; Stefanovits-Bányai, É. Changes in Total Polyphenol Content and Antioxidant Capacity of Stinging Nettle (*Urtica dioica* L.) from Spring to Autumn. *Period. Polytech. Chem. Eng.* **2020**, *64*, 548–554. [[CrossRef](#)]
33. Haya, S.; Bentahar, F.; Trari, M. Optimization of polyphenols extraction from orange peel. *J. Food Meas. Charact.* **2018**, *13*, 614–621. [[CrossRef](#)]
34. Yoon, H. Effects of aging on the phenolic content and antioxidant activities of magnolia (*Magnolia denudata*) flower extracts. *Food Sci. Biotechnol.* **2014**, *23*, 1715–1718. [[CrossRef](#)]
35. Lisiewska, Z.; Kmiecik, W.; Korus, A. Content of vitamin C, carotenoids, chlorophylls and polyphenols in green parts of dill (*Anethum graveolens* L.) depending on plant height. *J. Food Compos. Anal.* **2006**, *19*, 134–140. [[CrossRef](#)]
36. Kaur, A.; Kaur, M.; Kaur, P.; Kaur, H.; Kaur, S.; Kaur, K. Estimation and comparison of total phenolic and total antioxidants in green tea and black tea. *Glob. J. Bio-Sci. Biotechnol.* **2015**, *4*, 116–120.
37. Dimitrovska, M.; Tomovska, E.; Bocevska, M. Characterisation of Vranec, Cabernet Sauvignon and Merlot wines based on their chromatic and anthocyanin profiles. *J. Serbian Chem. Soc.* **2013**, *78*, 1309–1322. [[CrossRef](#)]
38. Cvejic, J.; Puškaš, V.; Miljić, U.; Torović, L.; Rakić, D. Varietal phenolic composition of Probus, Rumenika and Frankovka red wines from Fruka Gora (Serbia) and changes in main compounds during maceration. *Eur. Food Res. Technol.* **2016**, *242*, 1319–1329. [[CrossRef](#)]
39. Ebrahiminezhad, A.; Zare-Hoseinabadi, A.; Sarmah, A.K.; Taghizadeh, S.; Ghasemi, Y.; Berenjian, A. Plant-Mediated Synthesis and Applications of Iron Nanoparticles. *Mol. Biotechnol.* **2017**, *60*, 154–168. [[CrossRef](#)]
40. Machado, S.; Pinto, S.L.; Grosso, J.P.; Nouws, H.P.A.; Albergaria, J.T.; Delerue-Matos, C. Green production of zero-valent iron nanoparticles using tree leaf extracts. *Sci. Total Environ.* **2013**, *445–446*, 1–8. [[CrossRef](#)] [[PubMed](#)]
41. Chandini, S.K.; Rao, L.J.; Subramanian, R. Influence of extraction conditions on polyphenols content and cream constituents in black tea extracts. *Int. J. Food Sci. Technol.* **2011**, *46*, 879–886. [[CrossRef](#)]
42. Capparucci, C.; Gironi, F.; Piemonte, V. Equilibrium and extraction kinetics of tannins from chestnut tree wood in water solutions. *Asia-Pac. J. Chem. Eng.* **2011**, *6*, 606–612. [[CrossRef](#)]
43. Bae, S.; Hanna, K. Reactivity of Nanoscale Zero-Valent Iron in Unbuffered Systems: Effect of pH and Fe(II) Dissolution. *Environ. Sci. Technol.* **2015**, *49*, 10536–10543. [[CrossRef](#)]
44. Freyria, F.S.; Esposito, S.; Armandi, M.; Deorsola, F.; Garrone, E.; Bonelli, B. Role of pH in the Aqueous Phase Reactivity of Zerovalent Iron Nanoparticles with Acid Orange 7, a Model Molecule of Azo Dyes. *J. Nanomater.* **2017**, *2017*, 2749575. [[CrossRef](#)]
45. Hotze, E.M.; Phenrat, T.; Lowry, G.V. Nanoparticle Aggregation: Challenges to Understanding Transport and Reactivity in the Environment. *J. Environ. Qual.* **2010**, *39*, 1909–1924. [[CrossRef](#)]
46. Praetorius, A.; Badetti, E.; Brunelli, A.; Clavier, A.; Gallego-Urrea, J.A.; Gondikas, A.; Hasselov, M.; Hofmann, T.; Mackevica, A.; Marcomini, A.; et al. Strategies for determining heteroaggregation attachment efficiencies of engineered nanoparticles in aquatic environments. *Environ. Sci. Nano* **2020**, *7*, 351–367. [[CrossRef](#)]
47. Reddy, A.V.B.; Madhavi, V.; Reddy, K.G.; Madhavi, G. Remediation of Chlorpyrifos-Contaminated Soils by Laboratory-Synthesized Zero-Valent Nano Iron Particles: Effect of pH and Aluminium Salts. *J. Chem.* **2012**, *2013*, 521045. [[CrossRef](#)]
48. Ševců, A.; El-Temsah, Y.S.; Filip, J.; Joner, E.J.; Bobčíková, K.; Černík, M. Zero-valent iron particles for PCB degradation and an evaluation of their effects on bacteria, plants, and soil organisms. *Environ. Sci. Pollut. Res.* **2017**, *24*, 21191–21202. [[CrossRef](#)]
49. Wang, T.; Lin, J.; Chen, Z.; Megharaj, M.; Naidu, R. Green synthesized iron nanoparticles by green tea and eucalyptus leaves extracts used for removal of nitrate in aqueous solution. *J. Clean. Prod.* **2014**, *83*, 413–419. [[CrossRef](#)]
50. Devatha, C.P.; Thalla, A.K.; Katte, S.Y. Green synthesis of iron nanoparticles using different leaf extracts for treatment of domestic waste water. *J. Clean. Prod.* **2016**, *139*, 1425–1435. [[CrossRef](#)]
51. Mystrioti, C.; Xanthopoulou, T.D.; Tsakiridis, P.; Papassiopi, N.; Xenidis, A. Comparative evaluation of five plant extracts and juices for nanoiron synthesis and application for hexavalent chromium reduction. *Sci. Total Environ.* **2016**, *539*, 105–113. [[CrossRef](#)] [[PubMed](#)]
52. Ran, J.; Soliver, F.; Kjellerup, B.V. Remediation of Polychlorinated Biphenyls (PCBs) in Contaminated Soils and Sediment: State of Knowledge and Perspectives. *Front. Environ. Sci.* **2018**, *6*, 79. [[CrossRef](#)]
53. Horváthová, H.; Lászlóvá, K.; Dercová, K. Bioremediation of PCB-contaminated shallow river sediments: The efficacy of biodegradation using individual bacterial strains and their consortia. *Chemosphere* **2018**, *193*, 270–277. [[CrossRef](#)]
54. Horváthová, H.; Lászlóvá, K.; Dercová, K. Bioremediation vs. Nanoremediation: Degradation of Polychlorinated Biphenyls (PCBs) Using Integrated Remediation Approaches. *Water Air Soil Pollut.* **2019**, *230*, 204. [[CrossRef](#)]

- 
55. Reygaert, W.C. The antimicrobial possibilities of green tea. *Front. Microbiol.* **2014**, *5*, 434. [[CrossRef](#)]
  56. Bokare, V.; Murugesan, K.; Kim, Y.-M.; Jeon, J.-R.; Kim, E.-J.; Chang, Y.S. Degradation of triclosan by an integrated nano-bio redox process. *Bioresour. Technol.* **2010**, *101*, 6354–6360. [[CrossRef](#)]

**Disclaimer/Publisher’s Note:** The statements, opinions and data contained in all publications are solely those of the individual author(s) and contributor(s) and not of MDPI and/or the editor(s). MDPI and/or the editor(s) disclaim responsibility for any injury to people or property resulting from any ideas, methods, instructions or products referred to in the content.